DOI: 10.3969/j.issn.1673-3185.2017.02.001 **http:** // english.ship-research.com

Translated from: LUO T, WAN D C. Numerical analysis of viscous effect on ship rolling motions based on CFD[J]. Chinese Journal of Ship Research, 2017, 12(2): 1-11, 48.

Numerical analysis of viscous effect on ship rolling motions based on CFD

LUO Tian[1,2,3], *WAN Decheng*[1,2,3]

1 School of Naval Architecture, Ocean and Civil Engineering, Shanghai Jiao Tong University, Shanghai 200240, China

2 State Key Laboratory of Ocean Engineering, Shanghai Jiao Tong University, Shanghai 200240, China

3 Collaborative Innovation Center for Advanced Ship and Deep-Sea Exploration, Shanghai 200240, China

Abstract: During the ship design procedure, the analysis of ship rolling motions is of great significance because the rolling motions have extraordinary effects on the sea-keeping, maneuverability and stability of a ship. It is difficult to simulate rolling motions due to the effect of viscosity, which causes many nonlinear components in computation. As such, the potential theory used for other ship motions cannot be used for rolling motions. This paper simulates the rolling motions of the DTMB 5512 ship model and the ship transverse section of the S60 ship model with a naoe-FOAM-SJTU solver using the Reynolds Averaged Navier Stokes (RANS) method based on the OpenFOAM. The results of rolling motions are compared with the experimental data, which confirms the reliability of the meshes and results. For the ship transverse section of the S60 ship model, the damping coefficient is divided into three parts with the Euler and RANS methods: friction, vorticity and wave parts. For the DTMB 5512 ship model, the damping coefficient is also respectively analyzed, including the friction, vorticity, wave and bilge keel parts. The results in this paper show that the vorticity part accounts for the greatest proportion, while the friction part accounts for the least, and the bilge keels reduces the damping moment to a certain extent which shows the effect of rolling parameters on rolling motions and moments.

Key words: ship; rolling motions; damping coefficient; damping moment; RANS method; Euler method

CLC number: U661.3

0 Introduction

In modern ship design, it is very important to predict the ship rolling motions accurately. However, the viscous effect of flow field has a great influence on the ship rolling motions, which causes many nonlinear components in the computation of ship rolling motions so that the ship rolling motions can not be accurately predicted by the traditional potential flow theory.

Ship roll damping coefficient is a key factor to determine the accuracy of ship rolling prediction, and generally can be divided into 5 parts[1]: friction damping coefficient, wave damping coefficient, vortex damping coefficient, lift damping coefficient and appendage damping coefficient. This classification is convenient to study the influence of external factors on the different components of damping coefficient, but these 5 damping coefficients are assumed to be linearly correlated. For the 5 parts, Ikeda et al.[2-3] put forward the corresponding empirical formula according to the ship model test in 1977-1978. However, the efficiency of ship model test is not high, and the application range of empirical formula is limited,

Received: 2016-09-01

Supported by: National Natural Science Foundation of China (51379125, 51490675, 11432009, 51579145); Chang Jiang Scholars Program of China (T2014099); Program for Specially-appointed Professors (Orientalists) in Universities in Shanghai (2013022); VIV/VIM Program of the Ministry of Industry and Information for Numerical Tank Innovation Research (2016-23/09)

Author(s): LUO Tian, female, born in 1991, master candidate. Research interest: analysis of ship rolling motion in viscous flow field. E-mail: sky360652272@163.com

WAN Decheng (Corresponding author), male, born in 1967, Ph.D., professor. Research interest: basic theory and application of hydrodynamics and computational fluid mechanics of ship and ocean engineering. E-mail: dcwan@sjtu.edu.cn

so that these 2 methods can not be used in large-scale ship model rolling study.

Nowadays, with the rapid development of computer technology, Computational Fluid Dynamics (CFD)[4] has been widely used in ship related research. In the simulation analysis of ship rolling motion, scholars have carried out a series of studies one after another. Luca and Stefano[5] used CFD software to simulate the rolling motion of mono-hull ship, catamaran and small waterline area ship; Miller et al.[6] used the Reynolds Averaged Navier Stokes (RANS) method to predict the three-dimensional cylinder with bilge keel; Wilson et al.[7] used CFDSHIP-IOWA solver to predict the free rolling and forced rolling of ship under different speeds; Yang et al.[8] simulated the free and forced rolling motions of S60 ship model and calculated its damping coefficient. However, all of the above studies only obtained the total damping coefficient, or only separated the friction damping coefficient for analysis.

In this paper, the naoe-FOAM-SJTU solver[9], self-developed by the research group of the authors, is used to simulate the ship model motion and variation of flow field. The solver is developed based on open source software Open Field Operation and Manipulation (OpenFOAM)[10], which takes the RANS equation as the control equation, uses the finite volume method (FVM) to discrete the control equation, adopts the volume of fluid (VOF) technology to capture the free surface, closes the equation with SST k-ω turbulence model, and applies the Pressure-Implicit Split-Operator (PISO)[11] to obtain the coupling solution of velocity and pressure. However, the motion of hull is simulated by using the dynamic mesh technique and the six degrees of freedom motion solver. The naoe-FOAM-SJTU solver has been applied in the numerical simulation of complex flow problems such as ship engineering, offshore engineering and marine engineering, which includes various types of numerical wave generation and wave dissipation, ship-propeller-rudder matched self-propulsion and maneuvering motion, hydrodynamic performance of energy saving device, ship motion and viscous damping, wave slamming, floating platform motion and air gap, sloshing of liquefied natural gas (LNG) in liquid tanks, vortex-induced motion of Spar platform, and other complex problems. The relevant calculation results have been confirmed by a lot of experiments. Using this solver, Wu et al.[12] successfully predicted the open water performance of propeller; Shen et al.[13] obtained the generation method of an irregular wave; Li et al[14]. simulated the wake flows of wind turbine based on actuator line model; Yin et al.[15] simulated the resistance problem of real-scale VLCC ship; Cao et al.[16] simulated the multi-direction ocean wave problem; Zha et al.[17] simulated the wave-making resistance of catamaran; Shen et al.[18] simulated the self-propulsion of ship and the interaction of ship-propeller-rudder. The numerical simulation results above show that the naoe-FOAM-SJTU solver is reliable in solving the problems of ship and ocean engineering.

In this paper, Euler method and RANS method are used to simulate the forced rolling motion of transverse section of two-dimensional ship model, and the wave damping coefficient, friction damping coefficient and vortex damping coefficient are separated from the total damping coefficient. For the three-dimensional ship model, by comparing the rolling motions of bare hull with and without bilge keel, the friction damping coefficient and bilge keel damping coefficient are separated from the total damping coefficient. Because the rolling motion involved in this paper does not consider the influence of ship sway motion, the lift damping coefficient is not within the scope of analysis.

1 Numerical method

1.1 RANS method

For the naoe-FOAM-SJTU solver, the RANS equation is used as the control equation:

$$\nabla \cdot \boldsymbol{U} = 0 \tag{1}$$

$$\frac{\partial \rho \boldsymbol{U}}{\partial t} + \nabla \cdot \left(\rho\left(\boldsymbol{U} - \boldsymbol{U}_{\mathrm{g}}\right)\boldsymbol{U}\right) = -\nabla p_{\mathrm{d}} - g \cdot x \nabla \rho + \nabla \cdot \left(\mu_{\mathrm{eff}} \nabla \boldsymbol{U}\right) + (\nabla \boldsymbol{U}) \cdot \nabla \mu_{\mathrm{eff}} + \boldsymbol{f}_{\sigma} + \boldsymbol{f}_{\mathrm{s}} \tag{2}$$

where x is the location of mesh node; t is time; $\boldsymbol{U}$ is the velocity field; $\boldsymbol{U}_{\mathrm{g}}$ is the movement speed of mesh; $p_{\mathrm{d}} = p - \rho \boldsymbol{g} \cdot \boldsymbol{x}$, is the dynamic pressure; ρ is the density of liquid or gas; $\boldsymbol{g}$ is the vector of gravitational acceleration; $\boldsymbol{f}_{\sigma}$ is the surface tension term; $\boldsymbol{f}_{\mathrm{s}}$ is the source term; $\mu_{\mathrm{eff}} = \rho\left(\boldsymbol{v} - \boldsymbol{v}_{\mathrm{t}}\right)$ is the effective dynamic viscosity, in which $\boldsymbol{v}$ is the kinematic viscosity and $\boldsymbol{v}_{\mathrm{t}}$ is the vortex viscosity.

The SST $k-\omega$ turbulence model is used to close the control equation. The boundary compressible VOF method is used to track and capture the change of free surface. The transport equation is defined as follows:

$$\frac{\partial \alpha}{\partial t} + \nabla \cdot \left(\left(\boldsymbol{U} - \boldsymbol{U}_{\mathrm{g}}\right)\alpha\right) + \nabla \cdot \left(\boldsymbol{U}_{\mathrm{r}}(1-\alpha)\alpha\right) = 0 \tag{3}$$

where $\boldsymbol{U}_{\mathrm{r}}$ is the velocity field used to compress the

interface; α is the integral value and represents the volume proportion of fluid in the grid units, which is between 0 and 1:

$$\begin{cases}\alpha=0 & \text{Air}\\ \alpha=1 & \text{Water}\\ 0<\alpha<1 & \text{Interface}\end{cases} \tag{4}$$

The control equation is discretized by FVM method, namely, the computational domain is discretized into a series of small units and the computational flow field information is stored in the unit center of mesh. Finally, the value of the elemental area is obtained by interpolation of values of unit center. The PISO algorithm is used to conduct the iterative solution of the coupled equation of pressure and velocity after discretization, which is mainly composed of three steps: sub prediction, correction and re-correction. The specific steps and algorithms refer to Reference [9].

1.2 Euler method

In this paper, the Euler method is used to calculate the forced rolling of transverse section of two-dimensional S60 ship model. Because the friction damping coefficient and vortex damping coefficient are related to the viscosity of flow field and the wave damping coefficient is assumed to be independent of the viscosity of the flow field, the result obtained from the Euler method is wave damping coefficient.

The realization of Euler method is also based on the naoe-FOAM-SJTU solver. The value of the viscosity term in the solver can be set as 0, and the boundary conditions of the flow field can be changed to realize the Euler method, which is the same as that in Section 1.1.

1.3 Resistance coefficient in still water

In order to verify the feasibility of the Euler method and the independence between wave and viscosity, the Euler method and the RANS method are used to simulate the motion of KCS ship model in still water, and the still water resistance coefficient is solved.

The RANS method can be used to directly calculate the total resistance of the ship in the viscous flow field, and the resistance coefficient is obtained by:

$$C=\frac{F}{\frac{1}{2}\rho SV^2} \tag{5}$$

where F is the total ship resistance; S is the wetted surface area of the ship; and V is the speed.

The Euler method can only calculate the wave-making resistance coefficient C_w, and the friction damping coefficient C_f can be calculated by the 1957ITTC friction formula:

$$C_f=\frac{0.075}{\left(\lg Re^{-2}\right)^2} \tag{6}$$

where, the Reynolds number is $Re=VL/\nu$, and L is the length of ship. The final resistance coefficient is $C=C_f+C_w$.

1.4 Roll damping coefficient

In this paper, in order to compare with the experimental data, it is necessary to calculate the related roll damping coefficients. The calculation methods of the forced rolling and free roll damping coefficients are not consistent. The details are as follows.

1.4.1 Forced rolling

For forced rolling, the change of roll angle with time can be expressed as the following equation:

$$\theta=\theta_0\sin(\omega t) \tag{7}$$

where θ_0 is the initial roll angle, and ω is the roll frequency.

The roll damping moment can be expressed as:

$$\boldsymbol{M}=\boldsymbol{I}\ddot{\theta}+B\left(\dot{\theta}\right)\dot{\theta}+C(\theta,t) \tag{8}$$

where $\boldsymbol{I}$ is the total inertia moment; $B\left(\dot{\theta}\right)$ is damping coefficient, which can be approximated as:

$$B\left(\dot{\theta}\right)\approx B_{eq} \tag{9}$$

where B_{eq} is damping coefficient. If the restoring force coefficient $C(\theta,t)$ is assumed to be a polynomial of θ, then

$$C(\theta,t)=a_1\theta+a_2\theta^2+a_3\theta^3+\cdots+a_n\theta^n \tag{10}$$

When $\theta=0$, it can be derived that

$$B_{eq}=\frac{\boldsymbol{M}_0}{\theta_0\omega} \tag{11}$$

$$\hat{B}_{eq}=\frac{B_{eq}}{\rho\nabla B^2}\sqrt{\frac{B}{2g}} \tag{12}$$

where $\boldsymbol{M}_0$ is the damping moment of ship when the roll angle is 0°; B is the ship breadth.

From the above equations, it can be seen that for a certain working condition, the damping coefficient is related to the roll damping moment. Therefore, the roll damping moment can also be divided into 5 parts accordingly. For the visual analysis, this paper will give priority to the analysis of the roll damping moment curve and the maximum moment.

In this paper, the total damping moment obtained by naoe-FOAM-SJTU solver can be divided into 2 parts: shear and normal. The shear part is produced by the shear force around the hull, which is

the damping moment produced by the friction force, corresponding to the friction damping coefficient. The normal part is caused by the unbalanced pressure around the hull, which corresponds to the wave damping coefficient and the vortex damping coefficient. The assumption that the wave damping coefficient is independent of viscosity is gained from Euler method. Bilge keel increases the hull friction and changes the distribution and magnitude of vorticity around the hull. Therefore, it has an influence on both the shear part and the normal part. The relation of the 4 parts (vortex, wave, friction, appendage) of roll damping moment is as follows:

$$\begin{cases} \boldsymbol{M}_{\mathrm{p}} = \boldsymbol{M}_{\mathrm{pw}} + \boldsymbol{M}_{\mathrm{pe}} + \boldsymbol{M}_{\mathrm{pb}} \\ \boldsymbol{M}_{\mathrm{f}} = \boldsymbol{M}_{\mathrm{ff}} + \boldsymbol{M}_{\mathrm{fb}} \\ \boldsymbol{M} = \boldsymbol{M}_{\mathrm{p}} + \boldsymbol{M}_{\mathrm{f}} \end{cases} \tag{13}$$

where $\boldsymbol{M}_{\mathrm{p}}$ and $\boldsymbol{M}_{\mathrm{f}}$ are normal and shear parts of damping moment obtained by RANS method; $\boldsymbol{M}_{\mathrm{p}}$ is produced by the common impact of vortex, wave and bilge keel; $\boldsymbol{M}_{\mathrm{f}}$ is produced by friction part; $\boldsymbol{M}_{\mathrm{pw}}$ is the normal part of damping moment obtained by Euler method and is induced by the impact of wave; $\boldsymbol{M}_{\mathrm{pe}}$ is rolling moment produced by vortex; $\boldsymbol{M}_{\mathrm{pb}}$ is the normal part of rolling moment only produced by the bilge keel; $\boldsymbol{M}_{\mathrm{ff}}$ is the rolling shear moment produced by the friction of bare hull; and $\boldsymbol{M}_{\mathrm{fb}}$ is the rolling shear moment produced by the single friction of the bilge keel.

1.4.2 Free rolling

For free rolling motion, it is not only necessary to estimate the roll decay period by time history curve of roll angle, but also necessary to calculate the damping coefficient $\mu_{\phi\phi}$ of the free ship rolling motion by using the curve[19]. Fig. 1 shows the typical time history curve of roll angle.

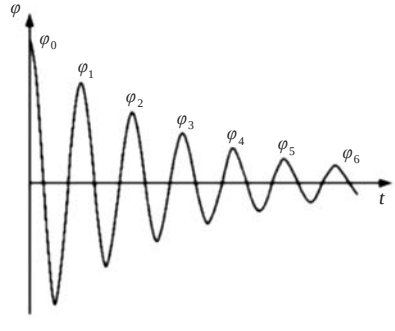

Fig.1 Time history curve of rolling angle

According to the ship seakeeping theory[20], the difference of two adjacent amplitudes $\Delta\varphi = \varphi_k - \varphi_{k+1}$ and the mean value $\varphi_m = (\varphi_k + \varphi_{k+1})/2$ can be obtained based on the curve. Taking φ_m as the horizontal axis and $\Delta\varphi$ as the vertical axis, the curve of damping coefficient can be obtained, as shown in Fig. 2.

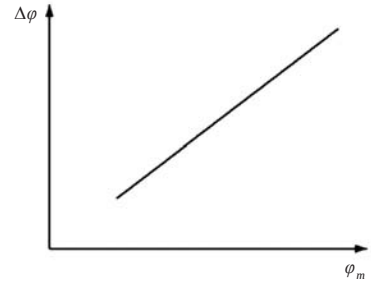

Fig.2 The curve of damping coefficient

Thus, the damping coefficient of free rolling can be gained through the following equation:

$$\mu_{\phi\phi} = \Delta\varphi/\pi \cdot \varphi_m \tag{14}$$

2 Computational models and meshes

In this paper, a total of 3 kinds of ship types are used: KCS, S60 and DTMB 5512. The computational meshes are generated by mesh generation tool SnappyHexMesh built-in OpenFOAM. In order to improve the computational accuracy, the free surface wave-making and the variation of vorticity near the hull are captured, and the meshes of the free surface and near the wall surface of the hull are properly densified. In addition, in order to achieve the ship rolling motions, the dynamic mesh technology is introduced in the calculation.

2.1 KCS ship type

When the feasibility of the Euler method is verified through the still water resistance, in order to compare with the experimental data[21], the same ship type in the experiment is used, namely, KCS ship type, and the parameters of KCS ship model are shown in Table 1.

Table 1 The main dimensions of KCS ship model

Parameter	Value
Ship length/m	7.36
Ship breadth/m	1.030 4
Draft/m	0.345 6
Block coefficient	0.651
Wetted surface area/m^2	9.757
Displacement volume/m^3	1.706
Center-of-gravity position/m	(3.79, 0, -0.113)

Fig. 3 shows the hull view of KCS ship model.

Fig.3 The KCS ship model

Due to the symmetry of the hull, the meshes are only divided at the starboard side of the longitudinal section of the ship model, and the sizes of the computational domain are: $-1.0L \leqslant x \leqslant 4.0L$, $0 \leqslant y \leqslant 1.5L$, and $-1.0L \leqslant z \leqslant 1.0L$. A total of 108×10^4 meshes are divided and the meshes of bow, stern and background are shown in Fig. 4.

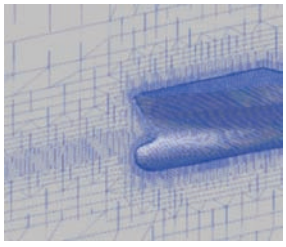

(a) The meshes of bow

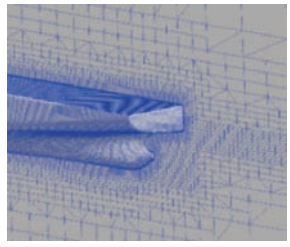

(b) The meshes of stern

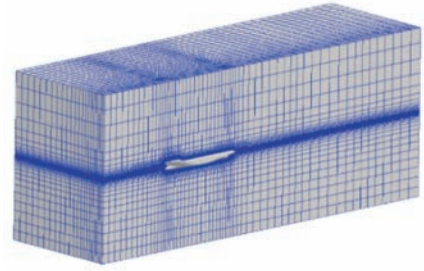

(c) Background meshes

Fig.4 Meshes distribution for KCS ship model

2.2 S60 ship type

For the typical transverse section of two-dimensional ship type discussed in the paper, in order to compare with the experimental data[22], this paper adopts the same ship type and section as in the experiment, namely, the typical transverse section of S60 ship type. The main parameters of S60 ship model are shown in Table 2.

Table 2 The main dimensions of S60 ship model

Parameter	Value
Ship breadth/m	0.237
Draft/m	0.096
Displacement volume/m^3	0.017 75

For the rolling simulation of transverse section of the two-dimensional ship model, the rolling axis is the x axis, and the axis O is the intersection of the center line of the transverse section of the ship and the waterline of the ship model when the transverse section is still. Size of the computational domain is: $-2.5B \leqslant y \leqslant 2.5B$ and $-2B \leqslant z \leqslant 2B$. In addition, the mesh convergence analysis is carried out for the rolling example, with the mesh number of 4×10^4, 7×10^4 and 14×10^4 respectively, as shown in Fig. 5.

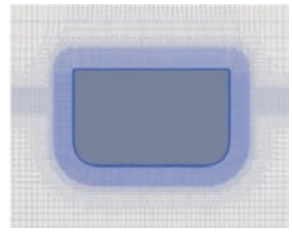

(a) Meshes 1(4×10^4)

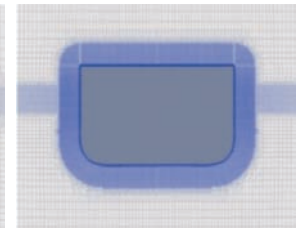

(b) Meshes 2(7×10^4)

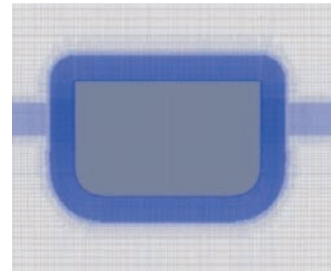

(c) Meshes 3(14×10^4)

Fig.5 Meshes distribution for S60 ship model

2.3 DTMB 5512 ship type

As for the typical three-dimensional ship type discussed in this paper, in order to compare with the experimental data, the same ship model is used, namely, DTMB 5512 ship model, and its key parameters are shown in Table 3.

Table 3 The main dimensions of DTMB 5512 ship model

Parameter	Value
Ship length/m	3.048
Ship breadth/m	0.409
Draft/m	0.132
Wetted surface area/m^2	1.397 63
Displacement volume/m^3	0.083
Center-of-gravity position/m	(1.524,0,0.03)

The bare hull models with and without bilge keel are shown in Fig. 6.

(a) The bare hull model

(b) The bare hull model with bilge keels

Fig.6 The DTMB 5512 ship models

For rolling motion, the rolling center coincides with the center of gravity, and the roll axis is the line parallel to the water plane and passing through the center of gravity on the central longitudinal section. Size of the computational domain is: $-1.0L \leqslant x \leqslant 3.0L$, $-2.0L \leqslant y \leqslant 2.0L$, $-1.0L \leqslant z \leqslant 0.5L$. In order to verify the reliability of the meshes, the mesh convergence is also verified. The number of meshes is 97.8×10^4, 232×10^4 and 646×10^4 respectively, among which the computational domain with 232×10^4 meshes is shown in Fig. 7.

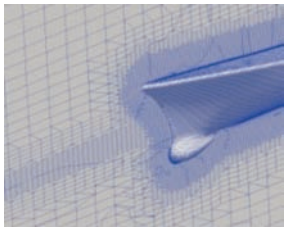

(a) The meshes of bow

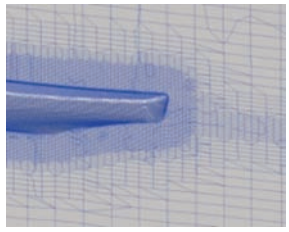

(b) The meshes of stern

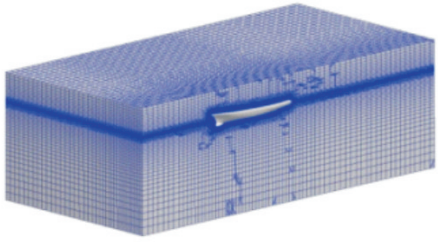

(c) Background meshes

Fig.7 Meshes distribution for DTMB 5512 ship model

3 Verification and calculation results

3.1 Rolling calculation of typical transverse section of two-dimensional S60 ship model

In this paper, Euler method and RANS method are used to simulate the forced rolling motion of the transverse section of two-dimensional S60 ship model. Finally, the roll damping moment is divided into 3 parts: wave, friction and vortex.

3.1.1 Feasibility verification of Euler method

In order to verify the feasibility of the Euler method and the accuracy of the wave prediction around the hull, the naoe-FOAM-SJTU solver is used in this paper. This paper uses RANS method and Euler method to calculate the still water resistances of ship under different Froude numbers *Fr*, which are compared with the experimental data. The results are shown in Table 4.

Table 4 The comparison between the results of two methods and the experimental data

Fr	Experimental data	Euler	Error/%	RANS	Error/%
0.25	3.574	3.705	3.66	3.529	1.26
0.27	4.006	4.180	4.34	4.029	0.58

It can be seen from Table 4 that the results obtained by the Euler method are close to the experimental results, namely, the wave-making damping part obtained by Euler method is reliable. This method can be used to calculate the wave damping moment in the roll damping moment.

When $Fr = 0.27$, the comparison of wave pattern calculated by the 2 methods is shown in Fig. 8, in which the upper part is the calculation result of Euler method and the lower part is the calculation result of RANS method.

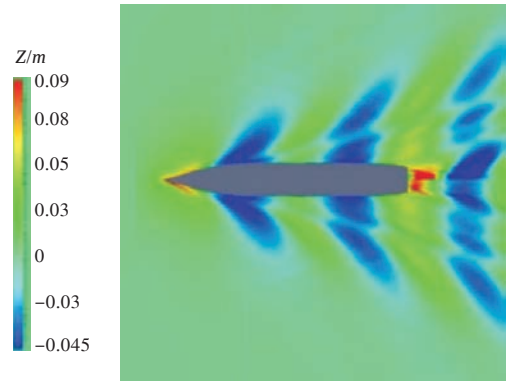

Fig.8 The comparison of wave pattern between Euler and RANS methods

It can be seen from the above resistance coefficients that the error between the results of the two methods and the experimental results is within the allowable range, indicating that the calculation results obtained by the Euler method are reliable for the non-viscous flow field. According to the stable wave patterns obtained by the Euler method and the RANS method, the wave patterns around the hull are almost the same. Therefore, it can be inferred that the viscous effect of the flow field does not have much influence on the wave-making near the hull. It can be further inferred that it is feasible to use the Euler method to calculate the wave damping part in the rolling simulation.

3.1.2 Feasibility verification of RANS method

In order to compare with the experimental data of Ikeda et al.[2-3], RANS method is used for the forced rolling calculation of the typical transverse section of two-dimensional S60 ship model under the same rolling condition. The rolling condition is shown in Table 5.

Table 5 The validation conditions of the method and mesh for forced roll motion with S60 ship model

Roll frequency/(rad·s^{-1})	5.274 5
Roll angle/rad	0.15, 0.17, 0.22, 0.25
Flow field density/(kg·m^{-2})	998.2
Gravitional acceleration/(m·s^{-2})	9.8
Kinematic viscosity of fluid/(m^2·s^{-1})	1.0×10^{-6}

Firstly, 0.17 rad is used to verify the convergence and the results are shown in Table 6.

Table 6 The validation results of convergence study of S60 ship model

Mesh	The number of meshes	$\hat{B}_{eq}$ obtained from the experiment	$\hat{B}_{eq}$	Error/%
Meshes 1	4×10^4	0.002 6	0.002 025	22.1
Meshes 2	7×10^4	0.002 6	0.002 378	8.5
Meshes 3	14×10^4	0.002 6	0.002 446	5.9

According to the data in Table 6, the error between meshes 2 and meshes 3 is within the allowable range. However, taking into account the efficiency, meshes 2 will be selected in the subsequent calculation.

In order to further verify the reliability of the calculation results of meshes 2, meshes 2 is selected for the forced rolling calculation under the other three roll angles, and the results are shown in Table 7.

Table 7 The validation results of damping coefficient for forced roll motion

θ_0/rad	Experimental result of Ikeda $\hat{B}_{eq}$	Calculation result of naoe-FOAM-SJTU $\hat{B}_{eq}$	Error/%
0.15	0.002 014	0.002 003	0.53
0.22	0.002 639	0.002 486	5.81
0.25	0.002 721	0.002 800	2.90

From the numerical results in Table 7, it can be seen that the errors are within the allowable range, and it can be confirmed that it is reliable to calculate the results of the forced rolling motion of the transverse section of two-dimensional ship model by adopting the RANS method and meshes 2.

3.1.3 Calculation results of the forced rolling motion of the typical transverse section of two-dimensional S60 ship model

In order to separately analyze the different components of roll damping coefficient during the forced rolling motion of the transverse section of the two-dimensional ship model, this paper uses the Euler method and the RANS method to simulate the ship rolling in the same rolling condition, as shown in Table 8.

Table 8 The calculation conditions for forced roll motion

Calculation condition	Motion state	Roll frequency/(rad·s^{-1})	Inflow velocity(Fr)	Roll angle/rad
2DFR	Forced rolling	15	0	0.25

Under this condition, Fig. 9 shows the time history curves of forced roll moment with S60 ship model.

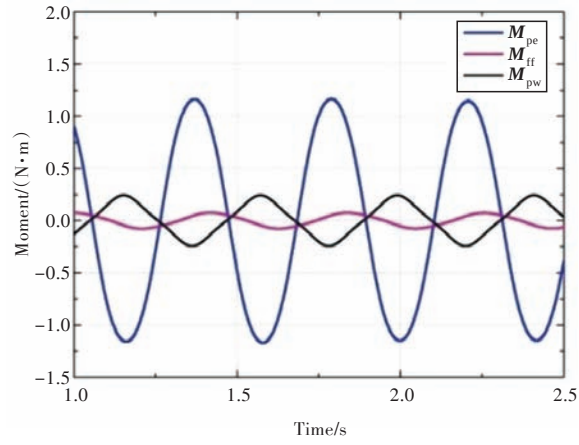

Fig.9 Time history curves of forced roll moment with S60 ship model

In Fig. 9, the black curve is the vertical portion $\boldsymbol{M}_{pw}$ of the moment of the ship calculated by the Euler method; the red curve is the friction moment $\boldsymbol{M}_{ff}$ of the ship calculated by the RANS method; the blue curve is the difference between $\boldsymbol{M}_{pw}$ and the vertical portion of the moment obtained by the RANS method, namely, $\boldsymbol{M}_{pe}$.

In viscous flow field, the vorticity distribution around the S60 ship model during the forced rolling motion is shown in Fig. 10.

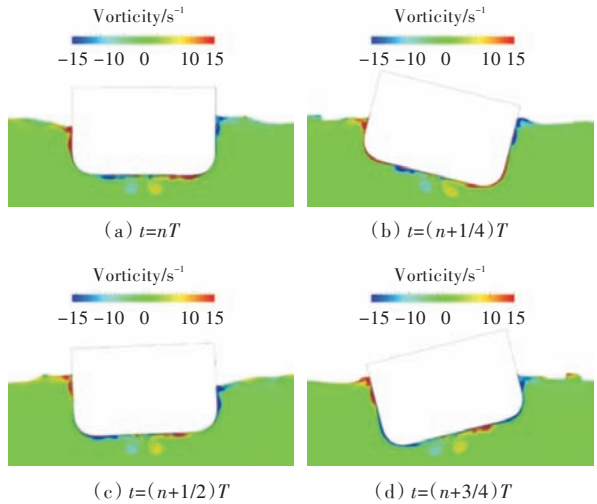

Fig.10 The vorticity distribution around the S60 ship model

Fig. 10 shows the vorticity distribution of four typical moments in the $(n-1)^{th}$ period, where T is the

forced roll period and t is the moment corresponding to the figure. The comparison of vorticity distribution between with viscosity and without viscosity during ship forced rolling is shown in Fig. 11.

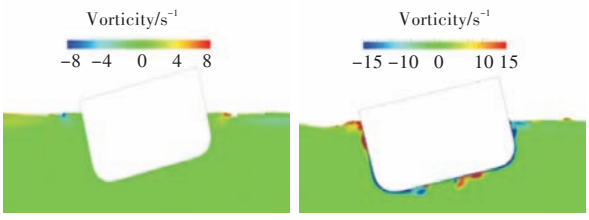

(a) Without viscosity (b) With viscosity

Fig.11 The comparison of vorticity distribution between viscosity and without viscosity

As can be seen from Fig. 9, the part influenced by vortex is much larger than the other parts in the forced roll damping moment. In the hull rolling process, a lot of vortices will emerge around the hull, resulting in uneven pressure around the hull. The moment produced by this part has a greater effect than that caused by friction and wave. At the same time, this result is similar to the experimental result of Ikeda et al.[2-3] and the numerical calculation result of Korpus et al.[23]. It is also worth noting that the direction of the moment generated by the wave part is opposite to that of the moment of the other two parts, and the reason analysis is shown in Fig. 12.

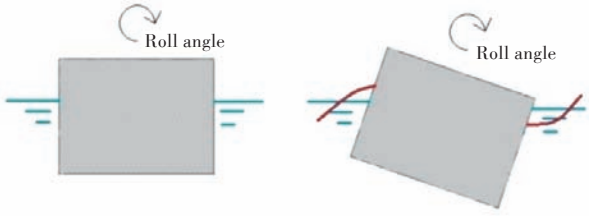

Fig.12 Analysis diagram of the wave damping moment

As seen from Fig. 12, the moment generated by the waves on the ship makes the ship move toward the overturning direction, which is opposite to the direction of the moment of the other two parts. However, because its proportion in the total moment is small, the direction of the total roll moment is the same with that of the roll moment generated by vortex.

In addition, it can be seen from the time history curves of moment (Fig. 9) that the time when the vortex damping and the friction damping parts reach the peak value and zero point is different. The peak time of the friction damping part is later than that of the vortex damping part. The vortex damping part of the ship model is determined by the specific state of the flow field when the transverse section of two-dimensional ship model rolls. From the above data, it can be seen that the peak value appears at the time when the roll angle is the largest. Corresponding to the vorticity diagram of the calculation results, it can be found that at this time, the vortices around the transverse section of the ship model are the most, especially at the bilge, resulting in extreme imbalance of the pressure around the ship. Thus, the vortex damping part of the moment reaches the peak. However, the friction damping part is determined by the relative velocity of the liquid near the transverse section of the ship model and the surface of the ship model. When transverse section of the ship model is at the maximum roll angle, the surface speed of the ship model is 0, while the nearby fluid still moves due to inertia. Afterwards, the ship model moves toward the opposite direction so that the relative velocity continues to increase, namely, the friction damping part of the moment will continue to increase. So, the peak of the friction damping part will appear later than that of the vortex damping part.

From the analysis of the ship rolling vorticity diagram (Fig. 10), it can be seen that vortex is generated on the wall of the transverse section of the two-dimensional ship model. When the roll angle of the ship model is gradually decreased from the maximum, the relative speed around the ship model begins to form a layer of thin vortex in certain direction. Thus, as the ship gradually turns left (or right), when the roll angle of ship model in the other direction reaches the maximum, the vortices in this direction have already been generated and attached to the hull surface to form a thicker layer. After that, the ship model rotates in the opposite direction and will immediately form vortices in the opposite direction around the ship model. Part of the outer vortices with different directions are neutralized and the non-neutralized part is discharged to the bottom and free surface along the bottom and side of the hull so that four vortex centers around the ship model are formed. The direction of the four vortices is determined by the initial rotation direction of the hull. When the initial rotation direction of the hull is changed, the direction of vortex will be reversed.

From the pressure and vorticity distributions in the non-viscous and viscous flow fields calculated from the Euler method and the RANS method (Fig. 11), it can be seen that the flow field without viscosity does not produce significant vorticity. Therefore, it can be confirmed that the vortex part of the damping coefficient is only affected by the viscos-

ity, namely, the vortex damping coefficient is obtained from the viscosity part of normal moment.

3.2 Rolling calculation of three-dimensional DTMB 5512 ship model

In this paper, the RANS method is used to simulate the rolling motion of DTMB 5512 three-dimensional ship type. Eventually, the friction damping part and the bilge keel damping part are separated from the total damping.

3.2.1 Calculation verification of free rolling of three-dimensional ship model

For the DTMB 5512 three-dimensional ship model, only the experimental results of free rolling in the stable speed are presented, so this section uses the same calculation conditions to simulate the free rolling of the ship model to verify the feasibility of RANS method and meshes. The calculation conditions are shown in Table 9. The results of convergence verification are shown in Table 10.

Table 9 The calculation condition of convergence study for free decay roll motion with DTMB 5512 ship model

Calculation condition	Motion state	Ship type	Inflow velocity(Fr)	Initial angle/rad
BHLS	Free decay	Without bilge keel	0.138	0.174

Table 10 The validation results of convergence study with DTMB 5512 ship model

Mesh	The number of meshes	Roll period obtained from the experiment/s	Roll period/s	Error/%	Damping coefficient obtained from the experiment	Damping coefficient	Error/%
Meshes 1	97.8×10^4	1.584	1.69	6.7	0.074 5	0.065 7	11.8
Meshes 2	232×10^4	1.584	1.65	4.2	0.074 5	0.070 3	5.6
Meshes 3	646×10^4	1.584	1.64	3.5	0.074 5	0.072 1	3.2

As seen from Table 10, the errors of meshes 2 and meshes 3 are within the allowable range. But, taking into account the efficiency, this paper will select meshes 2 in the subsequent calculation.

In order to further verify the reliability of the results obtained by using the method and the meshes, two kinds of inflow velocities are used for calculation and verification according to meshes 2 and experiment data. The two specific conditions are shown in Table 11.

Table 11 The calculation conditions for free decay roll motion with DTMB 5512 ship mode

Calculation condition	Motion state	Ship type	Inflow velocity(Fr)	Initial angle /rad
BHLS	Free decay	Without bilge keel	0.138	0.174
BHML	Free decay	Without bilge keel	0.280	0.174

The calculation results are shown in Fig. 13 and Table 12.

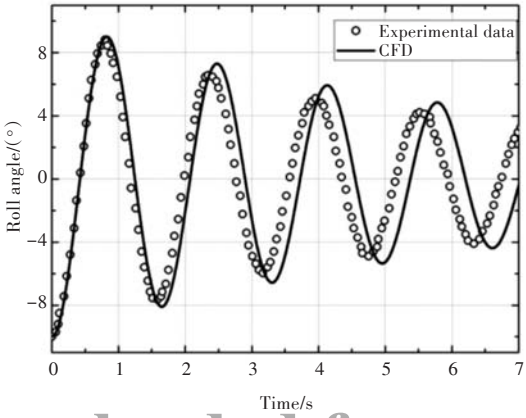

(a) BHLS

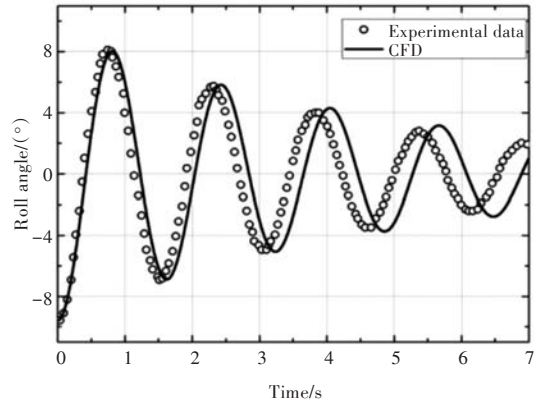

(b) BHML

Fig.13 The comparison of free decay roll motions simulation results and the experimental data with DTMB 5512

Table 12 The validation results for free decay roll motion with DTMB 5512 ship model

Calculation condition	Inflow velocity (Fr)	Roll period obtained from the experiment/s	Roll period/s	Error/%
BHLS	0.138	1.584	1.65	4.2
BHML	0.280	1.545	1.62	4.8

From the above results, it can be seen that the error between this calculation and experiment is within 6%, which proves that it is reliable to calculate the results of forced rolling motion of the transverse section of three-dimensional ship model by using RANS method and meshes 2. In addition, it can be seen from Fig. 13 that the relative error of roll period between the numerical simulation results and the experimental results is constant, but the absolute error

value will accumulate over time. In the time history curve of roll angle of free rolling, the error between the numerical simulation results and the experimental results is gradually increased over time.

3.2.2 Calculation results for forced rolling of three-dimensional DTMB 5512 ship model

In order to separately analyze the different components of the roll damping coefficient when the three-dimensional ship model is forced to move, the RANS method is used to simulate the bare hull model with and without bilge keel under the same working conditions. The specific conditions are shown in Table 13.

Table 13 The calculation conditions for forced roll motion with DTMB 5512 ship model

Calculation condition	Motion state	Ship type	Roll frequency /(rad·s^{-1})	Inflow velocity (Fr)	Roll angle/rad
BHFR	Forced rolling	Without bilge keel	6.28	0	0.25
BKFR	Forced rolling	With bilge keel	6.28	0	0.25

Under this working condition, the time history curves of forced roll moment are shown in Fig. 14.

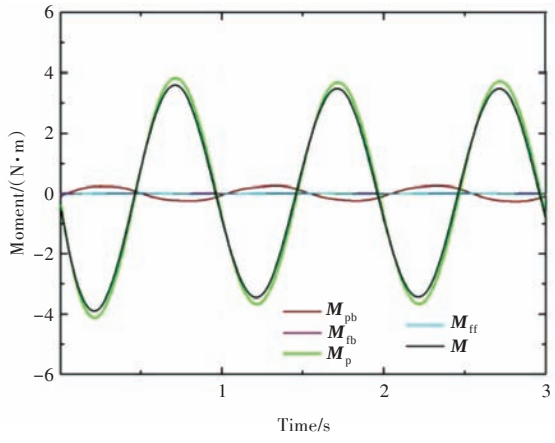

Fig.14 Time history curves of forced roll moment with DTMB 5512 ship model

In Fig. 14, the black line is the total moment $\boldsymbol{M}$ for the bare hull model with bilge keel; the green curve is the vertical part $\boldsymbol{M}_{pw}+\boldsymbol{M}_{pe}$ of the total moment acted on the bare hull model; the blue curve is the friction moment $\boldsymbol{M}_{ff}$ of the bare hull; the red curve is the vertical part $\boldsymbol{M}_{pb}$ of the moment affected by the bilge keel; the pink curve is the tangential part $\boldsymbol{M}_{fb}$ of the moment affected by the bilge keel.

In viscous flow field, when the ship is forced to roll, the vorticity distribution around the DTMB 5512 ship model is shown in Fig. 15.

As can be seen from the results in Fig. 15, in the forced rolling of the three-dimensional ship model, similar to the two-dimensional situation, the total roll damping moment is still dominated by $\boldsymbol{M}_{pw}+\boldsymbol{M}_{pe}$, while the proportions of the friction moments of the bare hull model with and without bilge

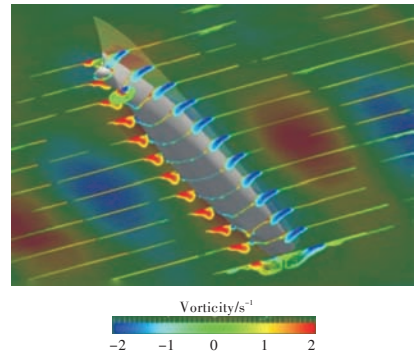

(a) Vorticity distribution when $\theta=0$ (bare hull)

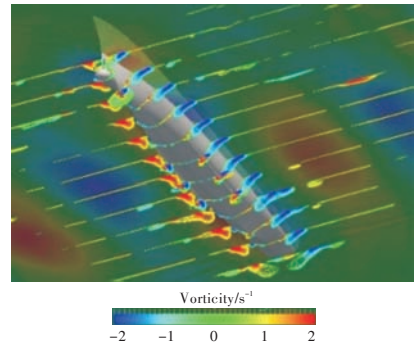

(b) Vorticity distribution when $\theta=0$ (bare hull with bilge keel)

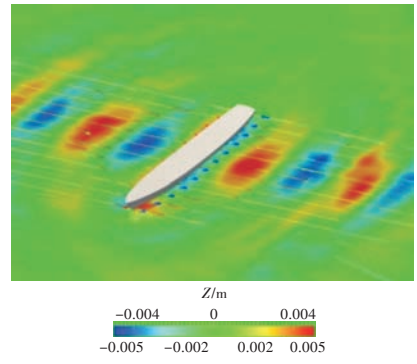

(c) Free surface when $\theta=0$ (bare hull)

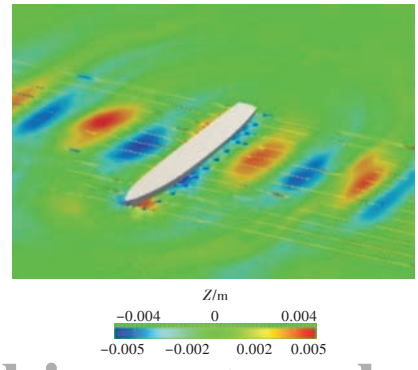

(d) Free surface when $\theta=0$ (bare hull with bilge keel)

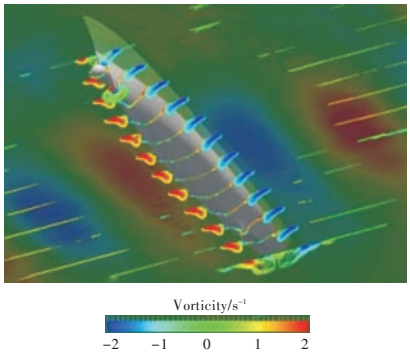

(e) Vorticity distribution when θ =0.25 rad(bare hull)

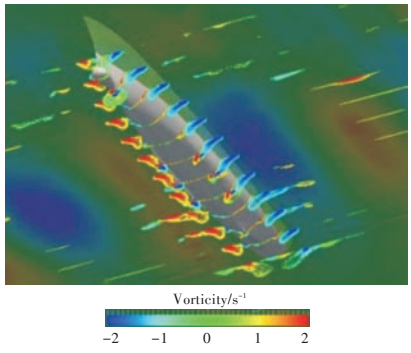

(f) Vorticity distribution when θ =0.25 rad(bare hull with bilge keel)

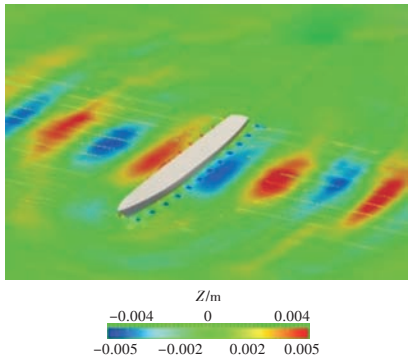

(g) Free surface when θ =0.25 rad(bare hull)

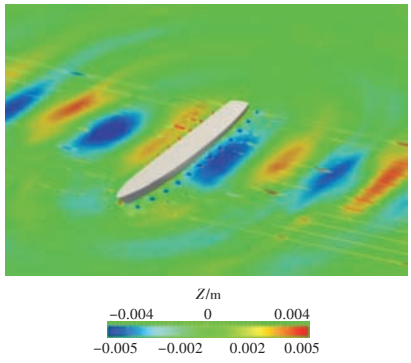

(h) Free surface when θ = 0.25 rad (bare hull with bilge keel)

Fig.15 The vorticity distribution around the DTMB 5512 ship model

keel are very small. It is also worth noting that, for the bare hull with bilge keel, the calculated total roll damping moment is reduced and the specific reason is shown in Fig. 16.

Reasons for the variation of damping moment caused by bilge keel mainly result from the two aspects: first, the bilge keel increases the surface area

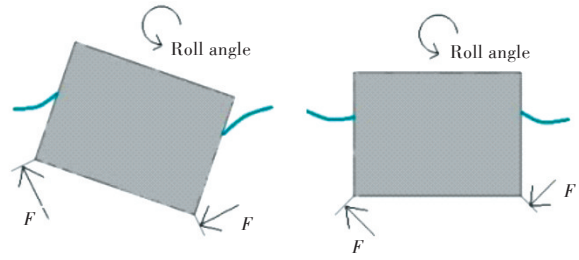

Fig.16 The influence of bilge keel on rolling motion

of the ship model, thereby increasing the friction damping; second, the bilge keel in the forced rolling of ship has a certain impact on the number and distribution of vortex in the flow field so that the roll damping moment of the ship is changed. Among them, the friction damping occupies a very small portion, which can be ignored in this analysis stage. The second factor firstly considers the damping moment caused by the pressure imbalance produced around the bilge keel. As shown in Fig. 16, when the ship model moves from the highest point to the balance position, the total damping moment is conducive to returning to the balance position for the ship model. But, at this time, the roll damping moment caused by the force of flow field faced by bilge keel prevents the ship model from returning to the balance position. Next, it can be seen from the vorticity diagram in Fig. 15 that, with consideration of bilge keel, two vortex centers are formed at the bilge of the hull, which changes the numerical value and distribution of vorticity in the flow field around the ship model. Under the combined effect of these two factors, the $\boldsymbol{M}_{\mathrm{p}}$ of ship model caused by the flow field is reduced within a certain range of roll angle, which also includes the maximum value of $\boldsymbol{M}_{\mathrm{p}}$.

Similar to the forced roll of transverse section of the two-dimensional ship model, a certain phase difference exists between the time history curve of friction damping moment and the time history curve of the vertical part of damping moment of the three-dimensional ship model. $\boldsymbol{M}_{\mathrm{p}}$ is related to the vorticity around the hull, and when the ship rolling reaches the maximum roll angle, the vorticity distribution near the ship model is the most uneven and the value of vorticity is the largest so that $\boldsymbol{M}_{\mathrm{p}}$ also reaches the maximum. When the ship model moves toward the opposite direction from the transverse section at the maximum roll angle, the velocity of the fluid relative to the surface of the ship model will continue to increase, namely, the shear force of moment will continue to increase. So, a certain phase difference exists between the two time history curves.

It can be also seen from Fig. 15 that the formation principle of vortex and vortex center near the ship model is similar to that of the transverse section of two-dimensional ship model. Vortex begins to form from the surface of the ship model when the ship is rolling. With the movement of the ship model, part of the vortices will be neutralized and dissipated with the newly formed vortices and part of the vortices will move outside under the influence of the movement of the ship model. Because the forced roll angle is slightly small in the example, the bare hull model eventually forms only two vortex centers, but the bare hull with bilge keel will form vortex center near the bilge keel. Fig. 15 also shows the change of free surface when the ship model rolls, from which it can be seen that the traveling waves formed by the bare hull model with and without bilge keel are basically similar.

4 Conclusions

In this paper, the RANS method is used to simulate the transverse section rolling of the two-dimensional S60 ship model, and the feasibility of meshes and the calculation method is verified. On the basis of this, combined with the calculation results of the Euler method under the same model and working condition, the ship damping coefficient is divided into three parts: friction, wave and vortex. The proportion of friction damping part in the total damping is the least, while that of vortex damping part is the largest. The correlation moments of the two have a certain phase difference. In addition, the direction of wave damping moment is opposite to those of friction and vortex damping moments.

This paper also uses the RANS method to simulate the free decay rolling motion of the three-dimensional DTMB 5512 ship model and verifies the feasibility of meshes and the calculation method. On this basis, the simulated calculation of the forced rolling motion for the three-dimensional bare hull model with and without bilge keel is carried out. The friction damping part and the bilge keel damping part are separated from the total damping for analysis. The results are similar to the two-dimensional results. The proportion of the friction damping part is very small, and the impact of wave and vortex damping is greater. The bilge keel within a certain roll angle range reduces the total damping moment, namely, a certain phase difference exists between the damping moment curve affected by the bilge keel part and the total damping moment curve.

In later studies, the effect of bilge keel on the free rolling motion of ship model will also be analyzed, and the Euler method will be applied to the forced rolling of three-dimensional ship model to separate the wave damping coefficient. At the same time, the influence of the relevant parameters change of ship rolling motion on the various parts of ship damping coefficient needs to be further studied.

References

[1] CHAKRABARTI S. Empirical calculation of roll damping for ships and barges[J]. Ocean Engineering, 2001, 28(7): 915-932.

[2] IKEDA Y, HIMENO Y, TANAKA N. On eddy making component of roll damping force on naked hull [J]. Journal of the Society of Naval Architects of Japan, 1977, 142: 54-64.

[3] IKEDA Y, HIMENO Y, TANAKA N. Prediction method for ship roll damping: 00405 [R]. Osaka: Department of Naval Architecture, University of Osaka, 1978.

[4] ALESSANDRINI B, DELHOMMEAU G. A fully coupled Navier-Stokes solver for calculation of turbulent incompressible free surface flow past a ship hull[J]. International Journal for Numerical Methods in Fluids, 1999, 29(2): 125-142.

[5] LUCA B, STEFANO B. Influence of viscosity on radiation forces: a comparison between monohull, catamaran and SWATH [C]//Proceedings of the Twenty-third International Offshore and Polar Engineering. Anchorage, Alaska, USA: International Society of Offshore and Polar Engineers, 2013.

[6] MILLER R, GORSKI J, FRY D. Viscous roll predictions of a circular cylinder with bilge keels [C]//Proceedings of the 24th Symposium on Naval Hydrodynamics. Fukuoka, Japan: NRNAS, 2002.

[7] WILSON R V, PATERSON E G, STERN F. Unsteady RANS CFD method for naval combatants in waves[C]// Proceedings of the 22nd ONR Symposium on Naval Hydrodynamics. Washington, DC: [s.n.], 2006.

[8] YANG C L, ZHU R C, MIAO G P, et al. Numerical simulation of rolling for 3-D ship with forward speed and nonlinear damping analysis [J]. Journal of Hydrodynamics, Series B, 2013, 25(1): 148-155.

[9] SHEN Z R, CAO H J, YE H X, et al. Manual of CFD solver naoe-FOAM-SJTU: 2012SR118110[P]. Shanghai: Shanghai Jiaotong University, 2012.

[10] JASAK H, JEMCOV A, ZELJKO T, et al. OpenFOAM: a C++ library for complex physics simulations [C]//International Workshop on Coupled Methods in Numerical Dynamics. Dubrovnik. Croatia: IUC, 2007: 1-20.

[11] ISSA R I. Solution of the implicitly discretised fluid flow equations by operator-splitting [J]. Journal of Computational Physics, 1986, 62(1): 40-65.

[12] WU J W, YIN C H, WAN D C. Numerical prediction of the propeller open-water performance based on

three numerical methods[J]. Chinese Journal of Hydrodynamics,2016,31(2):177-187 (in Chinese).
[13] SHEN Z R,WAN D C. An irregular wave generating approach based on naoe-FOAM-SJTU solver[J]. China Ocean Engineering,2016,30(2):177-192.
[14] LI P F,WAN D C,LIU J C. Numerical simulations of wake flows of wind turbine based on actuator line model[J]. Chinese Journal of Hydrodynamics,2016,31(2):127-134 (in Chinese).
[15] YIN C H,WU J W,WAN D C. Model- and full-scale VLCC resistance prediction and flow field analysis based on IDDES method[J]. Chinese Journal of Hydrodynamics,2016,31(3):259-268 (in Chinese).
[16] CAO H J,WAN D C. Development of multidirectional nonlinear numerical wave tank by naoe-FOAM-SJTU solver[J]. International Journal of Ocean System Engineering,2014,4(1):49-56.
[17] ZHA R S,YE H X,SHEN Z R,et al. Numerical computations of resistance of high speed catamaran in calm water[J]. Journal of Hydrodynamics,2014,26(6):930-938.
[18] SHEN Z R,WAN D C,CARRICA P M. Dynamic overset grids in OpenFOAM with application to KCS self-propulsion and maneuvering[J]. Ocean Engineering,2015,108:287-306.
[19] YANG B,SHI A G,WU M. Calculation of ship roll damping coefficient based on CFD[J]. Navigation of China,2012,35(3):76-80 (in Chinese).
[20] LI J D. Ship seakeeping[M]. Harbin: Harbin Engineering University Press,2007 (in Chinese).
[21] OLIVIERI A,PISTANI F,AVANZINI A,et al. Towing tank experiments of resistance,sinkageand trim,boundary layer,wake,and free surface flow around a naval combatant INSEAN 2340 model: IIHR-TR-421[R]. Iowa:The University of Iowa,2001.
[22] HUANG H,GUO H Q,ZHU R C,et al. Computations of ship roll damping in viscous flow[J]. Journal of Ship Mechanics,2008,12(4):568-573 (in Chinese).
[23] KORPUS R A,FALZARANO J M. Presiction of viscous ship roll damping by unsteady Navier-Stokes techniques[J]. Journal of Offshore Mechanics and Arctic Engineering,1997,119:108-113.

基于CFD的船舶横摇数值模拟与粘性效应分析

罗天[1,2,3], 万德成[1,2,3]

1 上海交通大学 船舶海洋与建筑工程学院,上海 200240
2 上海交通大学 海洋工程国家重点实验室,上海 200240
3 高新船舶与深海开发装备协同创新中心,上海 200240

摘　要:[**目的**]船舶横摇的准确预报对于船舶耐波性、稳性以及操纵性的研究具有十分重要的意义,但船舶横摇运动受流场粘性效应的影响很大,计算中存在较多非线性因素,因而并不适于常用于研究船舶运动的传统势流理论。为解决这一问题,[**方法**]采用基于OpenFOAM软件开发的naoe-FOAM-SJTU求解器,分别通过欧拉方法和RANS方法对S60船模典型二维横剖面的强迫横摇进行数值模拟,同时,模拟分析DTMB 5512不同三维船模的自由与强迫横摇运动。[**结果**]在成功将横摇阻尼力矩的不同成分分别计算出来后发现,其中漩涡阻尼所占的比例最大,摩擦阻尼所占的比例最小,而舭龙骨在一定的横摇角度范围内则减小了横摇阻尼力矩。[**结论**]该结果揭示了横摇参数对船舶横摇运动及横摇阻尼力矩的影响,对准确预报船舶的横摇运动具有重要意义。

关键词:船舶;横摇运动;阻尼系数;阻尼力矩;RANS方法;欧拉方法